

EFFECT OF RESIDUAL STRESS PROFILE ON HYDROGEN EMBRITTLEMENT SUSCEPTIBILITY OF PRESTRESSING STEEL

V. Kharin^(*) and J. Toribio^(**)

^(*)Institute of Applied Problems of Mechanics and Applied Mathematics of the National Academy of Sciences of Ukraine, Lviv, Ukraine

^(**)Department of Materials Engineering, University of Salamanca E.P.S., Campus Viriato, Avda. Requejo 33, 49022 Zamora, Spain
Tel: 980 545 000; Fax: 980 545 002, E-mail: toribio@usal.es

Abstract. The influence of the residual stress and strain distributions caused by surface treatments on the hydrogen embrittlement susceptibility of cold drawn prestressing steel wires, as characterized by means of the time to failure in the FIP test, is analysed. The model to predict the wire life in the hydrogenating aggressive solution is developed. It includes the simulation of hydrogen transport towards prospective rupture sites by diffusion affected by stress and plastic strain, as well as a criterion of critical hydrogen concentration to establish the fracture instant dependent on the stress-strain state. This allows one to analyse the influence of specific characteristics of the residual stress and plastic strain distributions, associated with different surface treatments, on the wire lives.

Resumen. Se analizan los efectos de las tensiones y deformaciones residuales, causadas por tratamientos superficiales, sobre la susceptibilidad a la fragilización por hidrógeno de aceros trefilados de pretensado, a través del tiempo de rotura en los ensayos de FIP. Se desarrolla el modelo para la predicción de la durabilidad de los alambres en la solución agresiva hidrogenante. Este incluye la simulación del transporte de hidrógeno hacia los futuros lugares de rotura por medio de la difusión asistida por las tensiones y la deformación plástica, complementada con un criterio de concentración crítica de hidrógeno para establecer el instante de rotura en función del estado tenso-deformacional. Esto permite analizar los efectos, sobre la durabilidad de los alambres, de las características particulares de las distribuciones de tensiones y deformaciones plásticas residuales, causadas por diferentes tratamientos superficiales.

1. INTRODUCTION

Prestressing of concrete structures with steel wires offers a powerful civil engineering technique aiming to introduce desirable stresses and to counterbalance undesirable ones so that the prestressing and service loading would produce stresses within specified limits [1]. Prestressing wires are usually made of eutectoid pearlitic steel heavily cold drawn to create elevated tensile properties. These wires, once subjected to high service stresses, remain such forever, usually in hostile environments, e.g., due to atmospheric humidity. All that makes them sensible to the presence of surface cracks, in particular those of stress corrosion origin.

Stress corrosion cracking of prestressing steel wires has been the subject of extensive studies which substantiated the important role of the hydrogen induced fracture (HIF) or hydrogen assisted cracking (HAC) in deterioration of reinforced concrete structures [2]. To evaluate the susceptibility of prestressing steels to stress corrosion cracking in general, and to HIF in particular, the International Federation for Prestressing (FIP) adopted the Ammonium Thiocyanate Test (ATT) for steel control [3]. However, despite being in use as a standard test method, it does not reveal neither how HIF goes on in prestressing steel wires nor the roles of various manufacturing and service factors. To this end, contributions to a better interpretation of the ATT and

understanding of hydrogen embrittlement development in prestressing steel are welcome to gain the capability of monitoring and improving the wires performance in hostile environments.

Residual stresses introduced by various manufacturing operations (machining, joining, heat-treating) and surface treatments (rolling, shot-peening, etc.) are known to be capable of influencing components strength and life through an introduction of residual stresses [4]. With regard to the hydrogen embrittlement of prestressing steel wires, the importance of residual stresses produced by rolling process has been demonstrated in terms of the wire lives in ATT solution [5]. In the case of HIF, the role of the residual stresses is potentially twofold. First, their mechanical effect, which is associated with *the magnitude* of residual stresses, is additive to the stresses caused by applied loading [4]. Besides, heterogeneous residual stress fields influence the hydrogen transportation rate towards prospective rupture sites in the wire by stress-assisted diffusion governed by *the gradient* of the hydrostatic component of stress [6]. Moreover, owing to the facts that residual stresses are produced by inhomogeneous plastic deformation [4] and that this latter itself also affects hydrogen diffusion in deformed metals [7-9], plastic strains caused by surface treatments must be taken into account as factors affecting the HIF susceptibility of wires, too.

Previous research [6] has established an important milestone providing quantitative relationship between the *level* of residual stress (represented by *hypothetical* residual stress distributions) and the fracture behaviour of prestressing steel wires under HIF conditions. However, detailed analysis of the influence of *realistic* residual stress and plastic strain profiles caused by different regimes of surface rolling on the HIF susceptibility of cold drawn prestressing steel wires has not been performed yet. This paper goes further in the analysis, so that the earlier developed model [6] is advanced and applied to analyse the influence of the residual stress-*and*-strain distributions after surface rolling on the hydrogen embrittlement susceptibility of cold drawn prestressing steel wires in FIP tests.

2. BACKGROUND THEORY

In general, HIF depends on the amount of hydrogen in prospective fracture sites in metal so that rupture events are associated with a critical combination of the responsible stress-strain field characteristics and hydrogen concentration *C* over a relevant material scale *x_c* (cell, "grain", or domain of interest), as described elsewhere [7-9]. HIF advances by hydrogen-assisted nucleation of a (micro)crack in the site of the locally worst "concentration-stress-strain" triple which may be resolved to define the critical concentration of hydrogen *C_{cr}* as follows:

$$C_{cr} = C_{cr}(\sigma_i, \epsilon_{pi}), \tag{1}$$

where $\sigma_i = \sigma_i(x)$ and $\epsilon_{pi} = \epsilon_{pi}(x)$ represent, respectively, the three principal components of stresses and plastic strains (*i* = 1,2,3) in a material point *x*. In particular cases of predominantly stress- or strain-controlled HIF, *C_{cr}* will be related to the corresponding single governing mechanical variable.

Hydrogen from corrosive environment penetrates into the metal and is accumulated in prospective fracture sites until its concentration *C(x,t)* attains the critical level *C_{cr}* after a certain time *t* which will be called time to failure *t_f* throughout his paper and this is when rupture event occurs. The criterion to determine fracture time *t_f* takes then the form:

$$C(x_c, t_f) = C_{cr}(x_c), \tag{2}$$

where a definite fracture locus *x_c* must be specified.

Although hydrogen transportation towards prospective damage sites comprises several consecutive stages [6-9], hydrogen diffusion in metal is often the slowest one which controls fracture time. In particular, this is considered to be the case under electrochemical hydrogenation, such as during ATT [6,7]. Diffusion in metals proceeds towards maximum system entropy which corresponds to uniform distribution of a given amount of a specie, represented by its concentration *C*, over available occupation sites whose density may be characterised by the solubility factor *K_s*. This latter

depends on the metal lattice dilatation induced by hydrostatic stress σ , and on the amount of lattice imperfections (traps for hydrogen, cf. Hirth [10]) dependent on the magnitude of equivalent plastic strain ϵ_p , which may be expressed as follows [7-9]:

$$K_s(\sigma, \epsilon_p) = K_{s\epsilon}(\epsilon_p) \exp(\Omega\sigma) \quad \text{with } \Omega = \frac{V_H}{RT}, \tag{3}$$

where *K_{sε}* is the strain-dependent component of solubility, *V_H* is the partial molar volume of hydrogen in metal, *R* the universal gas constant, and *T* the absolute temperature. This leads to the stress-strain affected diffusion flux [7-9]

$$\mathbf{J} = -D(\epsilon_p) \left\{ \nabla C - C \left[\Omega \nabla \sigma + \frac{\nabla K_{s\epsilon}(\epsilon_p)}{K_{s\epsilon}(\epsilon_p)} \right] \right\}, \tag{4}$$

where *D* is the diffusion coefficient of hydrogen in metal which characterises the specie mobility and depends, among other factors, on the lattice trap density, and thus on ϵ_p . Mass balance then gives the diffusion equation in terms of concentration in the form:

$$\frac{\partial C}{\partial t} = -\text{div } \mathbf{J}. \tag{5}$$

Hydrogen entry into metal, i.e. the boundary conditions for diffusion consistent with the role of diffusion as the rate-controlling step [7-9] and with the solubility expression (3) corresponds to the equilibrium between its environmental thermodynamic activity and hydrogen concentration within metal at the entry surface Γ :

$$C(\Gamma, t) = C_\Gamma \quad \text{with } C_\Gamma = C_e K_{s\epsilon}(\epsilon_p(\Gamma)) \exp(\Omega\sigma(\Gamma)), \tag{6}$$

where *C_e* is the equilibrium concentration of hydrogen in a virgin material (free of stress and strain) under given environmental conditions.

3. ANALYSIS OF HIF IN THE PRESTRESSING STEEL WIRES

3.1. Test Description

According to the FIP proposal [3], the ATT for hydrogen susceptibility evaluation of prestressing steels is performed by sustained loading of smooth round wires submerged in 20-wt.% aqueous solution of ammonium thiocyanate (NH₄SCN) and monitoring the time to fracture *t_f* vs. applied axial stress σ_{ap} .

The tests [5,6] to be considered in this paper were performed with prestressing steel wires of eutectoid high-strength steel which was cold drawn from a rod of initial diameter *d₀* = 12 mm to achieve the wire diameter *d* = 7 mm, and afterwards submitted to stress-relieve heat treatment with cooling in oil. The 0,2%-offset yield stress of a wire was $\sigma_{0.2}$ = 1435 MPa and the fracture toughness in an inert environment *K_{IC}* = 98 MPa√m [5,6]. A series of samples were tested in the as-

received condition (specimens C0), others were subjected to surface treatment by rolling process under loads of 80 and 260 N (specimens C8 and C26 respectively), cf. [5].

3.2. Distributions of Residual Stresses and Strains

To analyse the role of surface treatments on the hydrogen embrittlement susceptibility of wires, the data of X-ray diffraction measurements of the residual stresses and plastic strains inhomogeneity [5] were used. These results are available for the depths from the specimen surface up to 500 μm and mostly for the sole axial component σ_{zR} of the residual stresses, whereas analysis of hydrogen diffusion requires hydrostatic stress distributions along the wire radius $0 \leq r \leq a = d/2$. To fill in this deficiency, a reconstruction of the residual stresses was performed on the basis of these limited X-ray measurements for σ_{zR} stress in the wires under consideration [5]. Confining the analysis to the axisymmetric problem in cylindrical coordinates (r, θ, z) , the hoop residual stress $\sigma_{\theta R}(r)$ for the measured depths was estimated according to available axial residual stress distributions $\sigma_{zR}(r)$ using some similitude hypotheses derived from the analysis of the more representative sets of σ_{zR} and $\sigma_{\theta R}$ measurements in similar cases [4,5]. Then, for greater depths up to the wire axis, all stress distributions were extrapolated by quadratic parabolas satisfying the global equilibrium conditions over respective transverse and axial cross-sections. The radial stress $\sigma_{rR}(r)$ was evaluated afterwards from the reconstructed $\sigma_{\theta R}(r)$ distribution according to standard equilibrium equation which here reduces to the following

$$\frac{d(r\sigma_{rR})}{dr} = \sigma_{\theta R}. \quad (7)$$

Hydrostatic residual stresses $\sigma_R = (\sigma_{rR} + \sigma_{\theta R} + \sigma_{zR})/3$ obtained following this procedure are presented in Fig. 1. It is seen that the rolling process introduces severe inhomogeneity of residual stresses (samples C8 and C26) in contrast to relatively uniform distributions after drawing only (sample C0).

These nonuniform residual stresses are the consequences of the inhomogeneous near-surface plastic deformation due to rolling. The variation of the X-ray diffraction peak width was suggested as an indicator of the plastic strains inhomogeneity [5]. According to the reported measurements [5], plastic strain distribution after cold drawing without rolling is relatively homogeneous. Using the plastic incompressibility condition and the rod diameter reduction by cold drawing, the corresponding background level of the equivalent plastic strain in wires C0 may be estimated as $\epsilon_{p0} = 2\ln(d/d_0)$. Then, for the rolled wires C8 and C26 the equivalent plastic strain distributions were approximated from the corresponding X-ray data [5] in a rough piece-wise linear manner, as shown in Fig. 1.

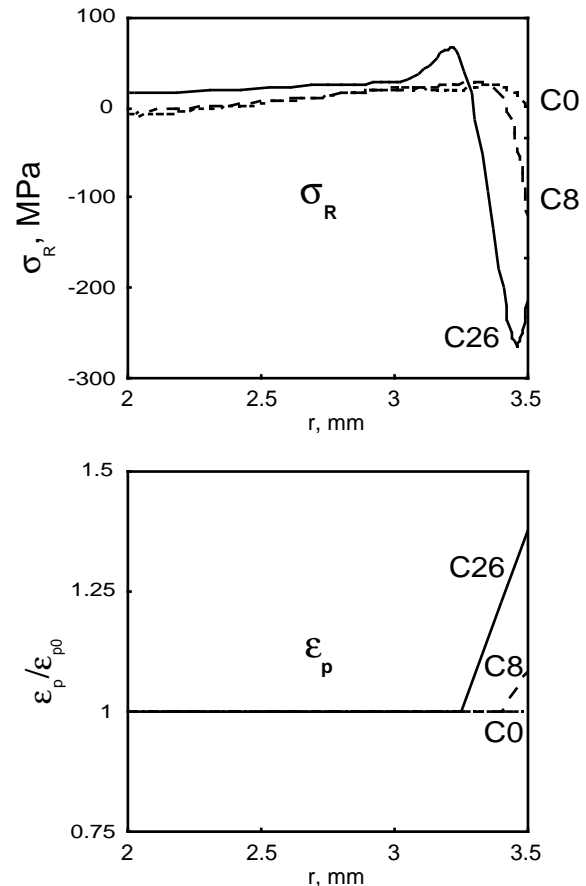


Fig. 1. Residual hydrostatic stress and plastic strain profiles in cold drawn wires C0 (dotted lines), C8 (dashed lines) and C26 (solid lines).

3.3. Model of Hydrogen Induced Fracture

With regard to fracture, the adopted model is basically the same as that proposed and substantiated in a previous paper [6]. The HIF criterion (2) is particularised so that fracture initiates—and the crack of a depth x_c is assumed to arise—when over a critical initiation scale x_c the average hydrogen concentration

$$\langle C(r,t) \rangle_{x_c} = \frac{1}{x_c} \int_{r-x_c}^a C(r,t) dr \quad (8)$$

attains the level $C_{cr}(\langle \sigma_{z,ef} \rangle_{x_c})$, where effective crack opening stress $\sigma_{z,ef}$ is the sum of the applied and the residual axial stresses, $\sigma_{z,ef} = \sigma_{ap} + \sigma_{zR}$, and its average value $\langle \sigma_{z,ef} \rangle_{x_c}$ is defined analogously to eqn (8). The subcritical crack growth phase from the size x_c to terminal rupture is neglected, which for high strength wires was shown to agree reasonably with experiments [6]. Accordingly, the fracture condition is expressed in terms of the critical value of stress intensity factor K_I :

$$K_I(x_c, \sigma_{z,ef}) = K_{IHAC}, \quad (9)$$

where K_{IHAC} is the critical stress intensity factor for hydrogen assisted cracking under given environmental conditions.

Fracture embryo is assumed to be a surface semi-elliptical crack with depth-to-width aspect ratio of 0.5. For arbitrary $\sigma_{z,ef}(r)$, the stress intensity factor values may be calculated using the weight function method [11]. However, for all considered $\sigma_{zR}(r)$ -distributions, which turned out here to be similar to the $\sigma_R(r)$ -paths shown in Fig. 1, in a relevant range of crack depths it was confirmed that with an error less than 5% K_I -values may be evaluated by means of the formula [6]

$$K_I = 0.94 \langle \sigma_{z,ef} \rangle_{x_c} \sqrt{\pi x_c} \quad (10)$$

Then, from equations (9) and (10), the critical scale for HIF is:

$$x_c = (1/\pi) [K_{IHAC} / (0.94 \langle \sigma_{z,ef} \rangle_{x_c})]^2 \quad (11)$$

Finally, the criterion for HIF may be established as the averaging of the relation (2) over the fracture scale x_c similarly to expression (8), so that the equation to predict the wire life t_f takes the form:

$$\langle C(r,t_f) \rangle_{x_c} = C_{cr}(\langle \sigma_{z,ef} \rangle_{x_c}) \quad (12)$$

This allows one to calculate t_f on the basis of the solution $C(r,t)$ of the problem of stress-strain assisted hydrogen diffusion of in a loaded wire during ATT.

4. WIRE LIFE PREDICTION

The model presented in the previous section points out the way to elucidate the role of residual stress-strain profiles (and of respective surface treatments) in HIF of wires, and to predict their time to fracture in hydrogenating environment. To apply the model to an analysis of ATT [5,6], a set of material properties must be specified. From the available experimental knowledge, the input data were chosen as follows.

The temperature was fixed to be $T = 323$ K. The partial molar volume of hydrogen in steels is known to be fairly constant, $V_H = 2$ cm³/mol [6,10]. With regard to the diffusion coefficient, wide dispersion of the measured data is proper at ambient temperatures for nominally the same alloys, as well as the hydrogen solubility data are also rather ambiguous, all of them being very sensitive to fine peculiarities of alloy composition and microstructure [10,12]. Quantitative information about their dependence on plastic strain is rare for most commercial alloys. Nevertheless, the following data may be accepted as reasonable estimations [6,12,13]:

$$D(\epsilon_p) = D_0 \exp(-\alpha \epsilon_p) \text{ with } \alpha = 2.9, \quad (13)$$

$$K_{SE}(\epsilon_p) = 1 + \beta \epsilon_p \text{ with } \beta = 4, \quad (14)$$

where D_0 is the diffusion coefficient in strain free ("as-received", before cold drawing) steel rod, $D_0 = 3 \cdot 10^{-12}$ m²/s at the given temperature. Finally, $K_{IHAC} = 0.27 K_{IC}$ [6] for commercial prestressing steel in the ATT solution.

To evaluate the left-hand part of the equation (12), the evolutions of hydrogen concentration in the samples can be determined in terms of dimensionless concentration $C(r,t)/C_e$ by solution of the problem of stress-strain assisted diffusion (4)-(6). Zero initial condition was taken here, i.e., $C(r,0) = 0$.

Numerical analysis of axisymmetrical stress-strain affected diffusion was implemented basically as described elsewhere [14] following the standard weighted residual process to built up a finite-element approximation of the initial-boundary value problem (4)-(6). In brief, applying the Galerkin process for the continuum discretised into finite elements, the same shape functions $\{W_m(r); m = 1,2,\dots,M\}$, M being the number of nodes in the mesh, served as trial and weighting functions, and also were used to approximate stress distributions $\sigma(r)$, diffusion coefficient (13) and solubility (14) dependent on plastic strain $\epsilon_p(r)$. Then, the weak form of the weighted residual statement of the problem rendered the system of differential equations with respect to time for the nodal values of concentration C . To solve it, the unconditionally stable Galerkin scheme of time-domain integration was employed. Simulations were performed using linear trial functions. Nonuniform spatial discretisation was employed to fit steep gradients of stress (see Fig. 1) and concentration. The smallest elements there were about 5 μ m length.

For all three residual stress-strain field profiles shown in Fig. 1, results of the diffusion computations together with equilibrium concentration distributions at $t \rightarrow \infty$ given by known steady-state solution of the problem $C_\infty(r)/C_e = K_S(\sigma(r), \epsilon_p(r))$ [7-9], are presented in Fig. 2. The effect of the rolling-induced stress-strain field is notable mostly in the near surface zone where the interaction of stress- and strain-controlled solubility terms (cf. equations (3), (13) and (14), and Fig. 1) causes respective concentration peaks. There is observed a slight delay of hydrogenation, which is increasing with more intense rolling due to the local decrease of diffusivity D at elevated plastic strains (i.e., traps density), cf. equation (13) and Fig. 1.

To predict theoretically wire lives in terms of plots of applied stress vs. time to fracture, the values of C_{cr} for respective wires were calculated according to the presented HIF model after diffusion simulations as the averages (8) of the obtained solutions $C(r,t)$ at the experimentally determined times of fracture in ATT solution of all three wires at some single load level, i.e., for $t = t_f$ available for all three wires at the same load level of $\sigma_{ap} = 1346$ MPa [5], as it is shown by squares in Fig. 3. Afterwards, the entire $\sigma_{ap}(t_f)$ -curves were reconstructed according to equation (12) using the results of the diffusion calculations and these C_{cr}

values, taken to be constants for the respective wires C0, C8 and C26 in a relatively narrow range of the applied stress under consideration. These curves are displayed in Fig. 3. The experimental data [6] obtained at various load levels for a steel nominally the same as C0 — but from another commercial stock — are also shown there.

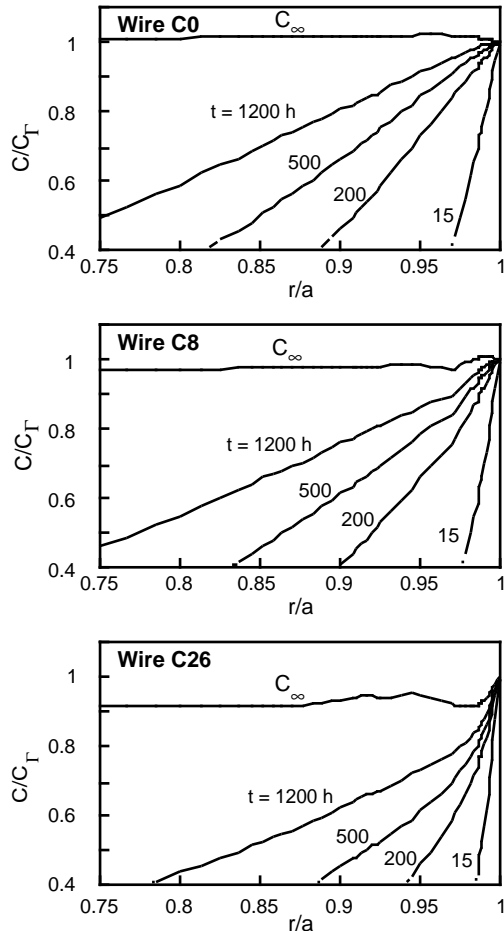


Fig. 2. Results of the stress-strain assisted diffusion computations for residual stress and plastic strain distributions in the wires C0, C8 and C26.

The agreement between the model predictions and the experimental results is satisfactory, so that the presented HIF model seems to be able to give reasonable predictions of prestressing steel lives under hydrogen embrittlement conditions with account for the role of residual stress profiles induced by surface treatment processes. The model provides a tool to analyse and explain their effect by the influence on the stress-and-strain assisted diffusion of hydrogen towards rupture sites.

Presented theory may be employed, in particular, to reduce the terms and costs of the experiments to evaluate the susceptibility of wires to hydrogen embrittlement by performing only limited short-term tests at elevated load levels, estimating from them the critical concentration C_{cr} , and then reconstructing the

entire curves σ_{ap} vs. t_f as described before. These theoretical curves must provide safe (low bound) life estimation for lower load levels. This is because at lower σ_{ap} actual critical concentrations may be only higher than the value of C_{cr} estimated theoretically from the elevated load data, and so the actual time to reach critical condition must be longer than the theoretical prediction. Obviously, adequate estimation of the diffusion coefficient D is crucial for the quantitative reliability of these predictions in absolute values, although this does not affect the evaluation of consequences of surface treatments in relative terms.

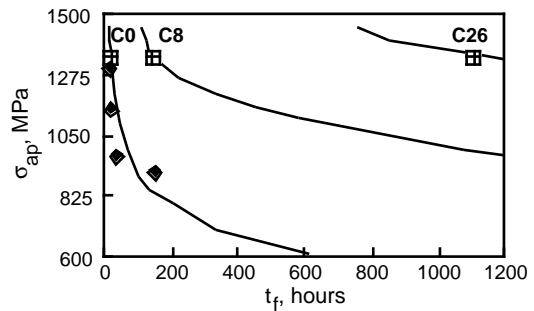


Fig. 3. Theoretical predictions of prestressing steel lives t_f vs. applied stress σ_{ap} in the ATT solution (curves for respective wires C0, C8 and C26 as indicated) and respective source data of single experiments [5] (squares); filled rhombs represent experimental data for a steel similar to C0 but obtained from a different commercial stock [6].

5. CONCLUSIONS

A model was developed to predict the life of high strength steel wires in ATT solution basing on the theory of stress-and-strain affected diffusion of hydrogen and on the stress-based criterion of hydrogen induced fracture.

The realistic residual stress and plastic strain profiles in the prestressing steels subjected to various surface treatments were reconstructed on the basis of X-ray diffraction measurements, and their effects on HIF susceptibility were calculated according to the proposed model. Satisfactory agreement with the available experimental results about time to failure in ATT solution was obtained.

Proposed computational model seems to be a promising tool to predict the lives of prestressing steel wires under HIF conditions on the basis of reduced testing, and to account for various residual stress and strain profiles induced by surface treatments.

Acknowledgements

The authors wish to thank the financial support of their research at the University of Salamanca provided by the

following institutions: Spanish Ministry for Scientific and Technological Research MCYT-FEDER (Grant MAT2002-01831), FEDER-INTERREG III (Grant RTCT-B-Z/SP2.P18), Junta de Castilla y León (JCYL; Grant SA078/04) and Spanish Foundation "Memoria de D. Samuel Solórzano Barruso".

REFERENCES

- [1] Valiente, A., Elices, M., "Premature failure of prestressed steel bars", *Engineering Failure Analysis*, 5, 219-227 (1998).
- [2] Bergsma, F., Boon, J.W., Etienne, C.F., "Détermination de la sensibilité des aciers précontrains à la fragilisation par l'hydrogène", *Revue Métallurgie*, 75, 153-164 (1978).
- [3] FIP-78. Stress Corrosion Test. Stress Corrosion Cracking Resistance for Prestressing Tendons. Techn. Rep. No. 5. FIP, Wexham Springs, Slough, UK (1981).
- [4] Macherauch, E., "Introduction to residual stress", In: *Advances in Surface Treatment*, Vol. 4, Oxford, 1-36 (1987).
- [5] Campos, J.M., Elices, M., "Tensiones residuales internas en alambres trefilados", *Anales de Mecánica de la Fractura*, 4, 143-157 (1987).
- [6] Toribio, J., Elices, M., "Influence of residual stresses on hydrogen embrittlement susceptibility of prestressing steels", *International Journal of Solids and Structures*, 28, 791-803 (1991).
- [7] Toribio, J., Kharin, V., "K-dominance condition in hydrogen assisted cracking: the role of the far field", *Fatigue and Fracture of Engineering Materials and Structures*, 20, 729-745 (1997).
- [8] Toribio, J., Kharin, V., "Evaluation of hydrogen assisted cracking: the meaning and significance of the fracture mechanics approach", *Nuclear Engineering and Design*, 182, 149-163 (1998).
- [9] Toribio, J., Kharin, V., "The effect of history on hydrogen assisted cracking: 1. Coupling of hydrogenation and crack growth", *International Journal of Fracture*, 88, 233-245 (1998).
- [10] Hirth, J.P., "Effects of hydrogen on the properties of iron and steel", *Metallurgical Transactions*, 11A, 861-890 (1980).
- [11] Fett, T., Munz, D., "Stress Intensity Factors and Weight Functions", *Computational Mechanics Publications*, Southampton-Boston (1997).
- [12] Coe, F.R., Moreton, J., "Diffusion of hydrogen in low-alloy steel", *Journal of the Iron and Steel Institute*, 204, 366-370 (1966).
- [13] Astiz, M.A., Álvarez, J.A., Guitiérrez-Solana, F., "Modelo numérico para analizar el efecto del hidrógeno sobre los procesos de fisuración dúctil", *Anales de Mecánica de la Fractura*, 15, 79-84 (1998).
- [14] Toribio, J., Kharin, V., "Role of fatigue crack closure stresses in hydrogen assisted cracking", In: *Advances in Fatigue Crack Closure Measurement and Analysis. Second Volume*, ASTM STP 1343, Philadelphia, PA, 440-458 (1999).